ISSN: 2710-0588

Vibration Isolation Performance Study of Shape Memory Alloy-Triple Spring Quasi-Zero-Stiffness System under Base Excitation

Lianjie Ding

College of Civil Engineering, Henan Polytechnic University, Jiaozuo, 454000, China

Abstract

In many critical scientific and engineering fields, controlling low-frequency vibrations is essential. The existing triple spring quasi-zero stiffness (QZS) isolator shows effective performance in low-frequency vibration control; however, its limited QZS range leads to reduced isolation bandwidth and deteriorated performance when structural displacement responses are large. To address this issue, this study proposes an improved QZS isolation system by partially replacing the vertical positive stiffness spring with a shape memory alloy (SMA) spring. The secondary stiffness characteristics and pseudoelasticity of the SMA spring are utilized to expand the QZS working range. The dynamic equations of the modified system, which exhibit piecewise nonlinear characteristics, are solved using the averaging method and validated numerically. The influence of various SMA parameters on the dynamic response of the improved system is analyzed. The results demonstrate that the SMA-enhanced triple spring QZS isolator exhibits a broader QZS range and superior low-frequency vibration isolation performance compared to the traditional triple spring QZS isolator.

Keywords

Low-frequency vibration isolation; shape memory alloy spring; triple spring quasi-zero stiffness isolation; amplitude-frequency characteristics.

1. Introduction

Low-frequency vibration issues in major engineering projects cannot be overlooked. For instance, large-scale power machinery such as steam turbines and marine internal combustion engines typically exhibit vibrations characterized by high amplitude and low frequency [1]. Therefore, it is essential to address low-frequency vibration isolation under base excitation. However, traditional linear passive vibration isolators struggle to simultaneously satisfy the conflicting requirements of load-bearing capacity and low-frequency vibration isolation. To address this challenge, researchers worldwide have proposed the concept of quasi-zero stiffness (QZS) vibration isolators, which exhibit the feature of "high static stiffness and low dynamic stiffness" [2].

As early as 1958, Molyneux et al. [3] optimized the structure of a positive-stiffness elastomer, enabling the passive vibration control system to achieve a low system stiffness while meeting high load-bearing requirements. Subsequently, Alabuzhev et al. [4] introduced a negative-stiffness device based on a linear spring and proposed the concept of quasi-zero stiffness. Platus [5], Peng Xian [6 - 8], Lee et al. [9], Santillan et al. [10], Han Junshu et al. [11] designed various quasi-zero stiffness systems by changing different negative-stiffness mechanisms and conducted nonlinear time-history and energy analyses on them. The results showed that these systems designed by changing negative-stiffness mechanisms have better performance in low-frequency vibration isolation. Later, Carrella et al. [12 - 13] designed a three-spring quasi-zero stiffness vibration isolator, which uses symmetrically arranged inclined springs to provide

ISSN: 2710-0588

negative stiffness and a vertical linear spring to provide positive stiffness, offering an effective solution for low-frequency vibration isolation.

However, the quasi-zero-stiffness stroke of the tri-spring quasi-zero-stiffness vibration isolator is relatively short, leading to a significant rightward shift of the amplitude-frequency response peak under strong excitation, resulting in a reduced vibration isolation bandwidth and weakened low-frequency vibration isolation performance. Current research primarily addresses this issue by modifying the damping and the mechanical characteristics of the negative stiffness mechanism. Nevertheless, improvements to the negative stiffness mechanism often complicate its design, while replacing linear damping with nonlinear damping poses additional challenges for damper design. Recently, scholars have proposed improvements to the tri-spring quasi-zero-stiffness vibration isolator by altering the mechanical properties of the positive stiffness spring. Chen et al. [14] introduced a quasi-zero-stiffness vibration isolator featuring a positive stiffness configuration composed of a pair of torsion springs, a rod, and linear bearings. Wang et al. [15] designed a compact tri-spring quasi-zero-stiffness vibration isolator using a permanent magnet structure as the negative stiffness mechanism and a wave spring as the positive stiffness. The studies on these improved quasi-zero-stiffness vibration isolators demonstrate that, compared to conventional tri-spring quasi-zero-stiffness vibration isolators, the enhanced designs can achieve a broader vibration isolation range while maintaining the load-bearing capacity and ultra-low system stiffness.

In this study, a shape memory alloy (SMA) spring is employed to replace part of the positive stiffness spring in the tri-spring quasi-zero-stiffness isolator (QZSI), resulting in a novel isolator termed the shape memory alloy-tri-spring quasi-zero-stiffness isolator (SMA-QZSI). The SMA-QZSI primarily leverages the secondary stiffness characteristics and pseudoelastic mechanical properties of the SMA spring to extend the quasi-zero-stiffness stroke of the tri-spring isolator, enhance its damping energy dissipation capacity, and maintain deformation suppression under large deformations. The average method is utilized to analytically solve the piecewise dynamic equations of the SMA-QZSI system, yielding the amplitude-frequency response equation. The dynamic behavior and low-frequency vibration isolation performance of this isolation system are investigated through numerical calculations, theoretical analysis, and experimental validation.

2. Working Principle of the SMA-QZSI System

2.1. Structure of the SMA-QZSI

The structure of the proposed SMA-QZSI is illustrated in Figure 1. This vibration isolator primarily comprises a positive stiffness component and a negative stiffness component. The positive stiffness component consists of a vertical linear spring and an SMA spring assembly. The SMA spring assembly integrates the following elements: a guide sleeve, upper cover, lower cover, actuator rod, blocking ring, upper tension disk, lower tension disk, and SMA springs. The negative stiffness component is mainly composed of a lateral spring, telescopic linkage, ring-type hinge support, pin shaft, and vertical column.

ISSN: 2710-0588

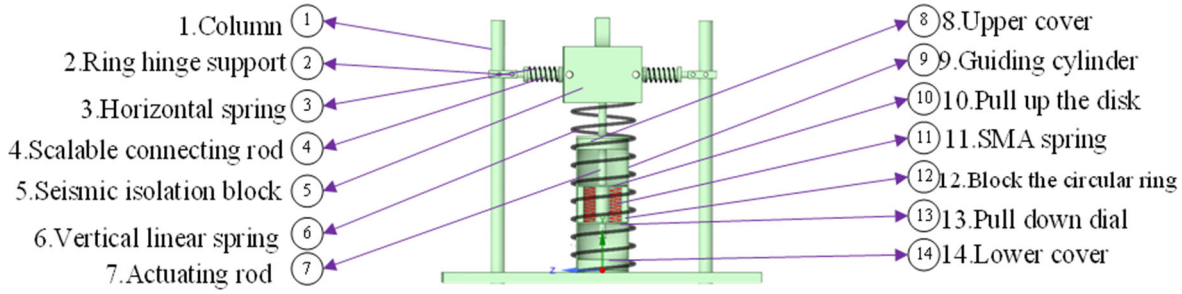

Figure 1. Structure of SMA-QZSI

2.2. Working principle of SMA-QZSI

According to the structure of the classic three spring quasi zero stiffness isolation device, its overall stiffness is composed of two parts: positive stiffness and negative stiffness. As shown in Figure 2 (a), the positive stiffness of QZSI is provided by linear springs, and the negative stiffness is provided by transverse springs. Therefore, it can be designed to exhibit zero stiffness at the equilibrium position. However, such a design can lead to the problem of low stiffness and weak bearing capacity when the isolator is under static load or small deformation. When the displacement of the isolator is large, the stiffness of the transverse spring will change from negative stiffness to positive stiffness, and the overall stiffness of the isolator will significantly increase, affecting the isolation performance. The seismic isolator proposed in this article can improve this situation through reasonable design. As shown in Figure 2 (b), due to the low secondary stiffness characteristics of SMA springs, when connected in parallel with positive stiffness springs, the displacement range of the isolator with quasi zero stiffness properties can be widened. When the displacement of the isolation object continues to increase, the stiffness of the SMA spring increases again, which can play a role in suppressing displacement under large deformations.

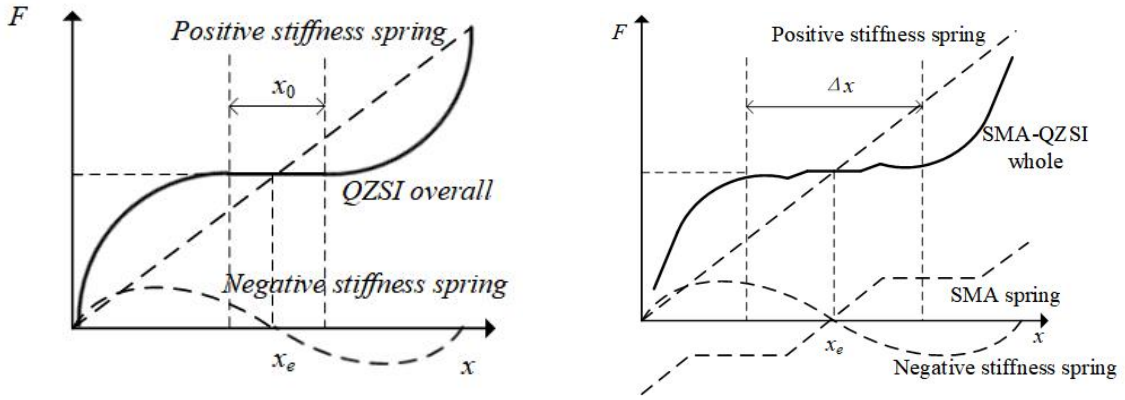

(a)QZSI (b)SMA-QZSI

Figure 2. Composition of force displacement relationship between QZSI and SMA-QZSI

2.3. Mechanical Model of SMA-QZSI

Figure3(a) shows the mechanical model of the SMA-QZSI system under basic excitation, where n represents the proportion of positive stiffness provided by the initial stiffness of the SMA spring in the system. Figure3(b) shows the force displacement relationship of the SMA spring device. Due to the special configuration of the damper, the SMA spring is in a tensile state regardless of whether it is in tension or compression. Therefore, the force displacement relationship of the SMA spring device has a center symmetry relationship as shown in the figure.

ISSN: 2710-0588

In Figure3(b) $k_{sma}(x)$ representing the stiffness of SMA at different deformation stages,x_{ms} representing the displacement of SMA at the beginning of martensitic transformation,x_{mf} indicating the end displacement of SMA martensitic transformation, x_{as} represents the displacement at the beginning of SMA martensitic reverse phase transformation,x_{af} indicate the displacement at the end of SMA martensitic reverse phase transformation.f_{ms}、f_{mf}、f_{as}、f_{af} indicate the corresponding restoring force.k_{sm1}、k_{sm2}、k_{sm3}、k_{sm4} indicate the stiffness of the corresponding stage. The pattern in the third quadrant is the same as it.

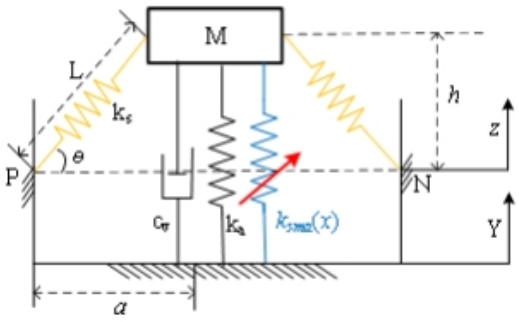

(a) The dynamic model of SMA-QZSI

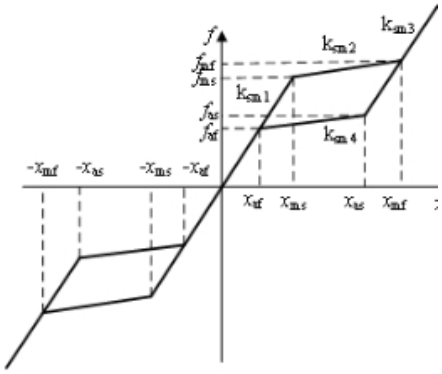

(b) The constitutive model of SMA

Figure 3. SMA-QZSI dynamic model and SMA mechanics displacement relationship

3. SMA-QZSI Dynamic Performance Analysis

This chapter establishes dynamic equations based on the established SMA-QZSI dynamic model, and then solves the dynamic equations using the averaging method to derive the amplitude frequency response equation and displacement transfer rate expression of the isolation system, and conducts parametric research.

3.1. Establishment of SMA-QZSI kinetic model

Based on Figure 3 (a) and the D'Alembert principle, the dynamic equation of the isolation system can be derived, namely:

$$m\ddot{z} + c_v\dot{z} + F_f = mY\omega^2\cos(\omega t) \tag{1}$$

ISSN: 2710-0588

$$F_{\mathrm{f}}=2k_{\mathrm{s}}(1-\frac{L}{(z^2+a^2)^{\frac{1}{2}}})z+k_{\mathrm{a}}z+F_{\mathrm{sma}} \tag{2}$$

Equation (1) is the desired dynamic equation, where m is a quality block M the quality, Y is the amplitude of the fundamental excitation given, z is the relative displacement of the mass block under basic excitation, c_{v} is damping, ω is excitation frequency. In equation (2), F_{f} is the restoring force exerted on the mass block under basic excitation, k_{s} is the stiffness of the transverse spring. a is the length of the transverse spring when it is horizontally compressed, k_{a} is the vertical linear spring stiffness, and $k_{\mathrm{v}}=k_{\mathrm{sm1}}+k_{\mathrm{a}}$， , then $k_{\mathrm{sm1}}=nk_{\mathrm{v}}$.L is the original length of the transverse spring, and F_{sma} is the restoring force of the SMA spring.The relationship between the excitation frequency ω and the natural frequency ω_0 of the system can be set as $\omega^2=\omega_0{}^2(1+\varepsilon\sigma_1)$， where $\varepsilon\sigma_1$ is a small positive quantity. Therefore, equation (1) can be written as:

$$m\ddot{z}+c_{\mathrm{v}}\dot{z}+F_{\mathrm{f}}+m\omega^2 z=mY\omega^2\cos(\omega t)+m\omega_0^2(1+\varepsilon\sigma_1)z \tag{3}$$

Substitute equation (2) into equation (1) and let $\alpha_1=k_{\mathrm{s}}/k_{\mathrm{v}}$, $\gamma=\mathrm{a}/\mathrm{L}$, $\zeta=c_{\mathrm{v}}/2m\omega_0$, $f_{\mathrm{f}}=F_{\mathrm{f}}/k_{\mathrm{v}}\mathrm{L}$, $\overline{z}=z/\mathrm{L}$, $\tau=\omega_0\mathrm{t}$, $\lambda=\omega/\omega_0$, $\eta=Y/\mathrm{L}$, $f_{\mathrm{sma}}=F_{\mathrm{sma}}/k_{\mathrm{v}}\mathrm{L}$, by nondimensionalizing and organizing equation (3), we can obtain:

$$\ddot{\overline{z}}+\lambda^2\overline{z}=-2\zeta\dot{\overline{z}}-(1-n)\overline{z}-f_{\mathrm{sma}}+2\alpha_1\overline{z}(\frac{1}{\sqrt{\gamma^2+\overline{z}^2}}-1)+\lambda^2\eta\cos(\lambda\tau)+(1+\varepsilon\sigma_1)\overline{z} \tag{1}$$

In order to facilitate the analytical solution of the dynamic equations, the nonlinear terms in the vicinity of $\overline{z}=0$ are approximated by Taylor series expansion $\overline{z}-\frac{\alpha_1}{\gamma^3}\overline{z}^3+\frac{3\alpha_1}{4\gamma^5}\overline{z}^5-\frac{5\alpha_1}{8\gamma^7}\overline{z}^7$,equation (4) can be rewritten as:

$$\ddot{\overline{z}}+\lambda^2\overline{z}=-2\zeta\dot{\overline{z}}-(1-n)\overline{z}-f_{\mathrm{sma}}-H_0+\lambda^2\eta\cos(\lambda\tau)+(1+\varepsilon\sigma_1)\overline{z} \tag{2}$$

Among them: $H_0=-\overline{z}+\frac{\alpha_1}{\gamma^3}\overline{z}^3-\frac{3\alpha_1}{4\gamma^5}\overline{z}^5+\frac{5\alpha_1}{8\gamma^7}\overline{z}^7$

3.2. Average method for solving

Let the main resonance response of the system be solved as:

$$\overline{z}=A\cos(\lambda\tau+\varphi) \tag{3}$$

Among them :A Expressing amplitude, φ indicates phase difference. Order $\Phi=\lambda\tau+\varphi$, according to the average method, solve equation (5) as follows:

$$\frac{\mathrm{d}A}{\mathrm{d}\tau}=-\frac{\int_0^{2\pi}\left[-2\zeta\dot{\overline{z}}-(1-n)\overline{z}-f_{sma}-H_0+\lambda^2\eta\cos(\lambda\tau)+(1+\varepsilon\sigma_1)\overline{z}\right]\sin\Phi d\Phi}{2\pi\lambda} \tag{4}$$

ISSN: 2710-0588

$$\frac{\mathrm{d}\varphi}{\mathrm{d}\tau}=-\frac{\int_0^{2\pi}\left[-2\zeta\dot{\bar{z}}-(1-n)\bar{z}-f_{sma}-H_0+\lambda^2\eta\cos(\lambda\tau)+(1+\varepsilon\sigma_1)\bar{z}\right]\cos\Phi d\Phi}{2\pi A\lambda} \tag{5}$$

Substitute equation (6) into equations (7) and (8), and let $\frac{\mathrm{d}A}{\mathrm{d}\tau}=\frac{\mathrm{d}\varphi}{\mathrm{d}\tau}=0$,The amplitude frequency response equation can be obtained:

$$4A^2\left(B_\varphi+F-\frac{\lambda^2}{2}-\frac{n}{2}\right)^2+\left(2\zeta A\lambda-2B_{\mathrm{A}}\right)^2=\lambda^4\eta^2 \tag{9}$$

At the same time, the displacement transfer rate of the system can be solved, that is:

$$TD=\frac{\sqrt{\eta^2+A^2+2A\eta\cos\varphi}}{\eta} \tag{6}$$

Among them : $F=\frac{3}{8}\frac{\alpha_1}{\gamma^3}A^2-\frac{15}{64}\frac{\alpha_1}{\gamma^5}A^4+\frac{175}{1024}\frac{\alpha_1}{\gamma^7}A^6$

$$B_{\mathrm{A}}=\frac{1}{2\pi}\int_0^{2\pi}\left(f_{\mathrm{sma}}\sin\Phi\right)\mathrm{d}\Phi=\begin{cases}B_{\mathrm{A1}},0\le A<x_{\mathrm{ms}}\\B_{\mathrm{A2}},x_{\mathrm{ms}}\le A\le x_{\mathrm{mf}}\end{cases}$$

$$B_{\mathrm{A1}}=0$$

$$B_{\mathrm{A2}}=\frac{(k_{\mathrm{sm1}}-k_{\mathrm{sm2}})(x_{\mathrm{ms}}-x_{\mathrm{af}})}{\pi}\left(\frac{x_{\mathrm{ms}}}{A}-1\right)$$

$$B_\varphi=\frac{1}{2A\pi}\int_0^{2\pi}\left(f_{\mathrm{sma}}\cos\Phi\right)\mathrm{d}\Phi=\begin{cases}B_{\varphi1},0\le A<x_{\mathrm{ms}}\\B_{\varphi2},x_{\mathrm{ms}}\le A\le x_{\mathrm{mf}}\end{cases}$$

$$B_{\varphi1}=\frac{n}{2}$$

$$B_{\varphi2}=[\frac{k_{\mathrm{sm2}}-k_{\mathrm{sm1}}}{2A\pi}\sqrt{\frac{(x_{\mathrm{ms}}-x_{\mathrm{af}})(2A-x_{\mathrm{ms}}+x_{\mathrm{af}})}{A^2}}(A-x_{\mathrm{ms}}+x_{\mathrm{af}})$$
$$-A\arccos\left(\frac{A-x_{\mathrm{ms}}+x_{\mathrm{af}}}{A}\right)+A\arccos\left(\frac{x_{\mathrm{af}}}{A}\right)$$
$$-x_{\mathrm{ms}}\sqrt{\frac{A^2-{x_{\mathrm{ms}}}^2}{A^2}}-x_{\mathrm{af}}\sqrt{\frac{A^2-{x_{\mathrm{af}}}^2}{A^2}}+A\arccos\left(\frac{x_{\mathrm{ms}}}{A}\right)]+\frac{n}{2}$$

$$\cos\varphi=2A(B_\varphi+F-\frac{\lambda^2}{2}-\frac{n}{2})/\eta\lambda^2$$

3.3. Comparison of Vibration Isolation Performance between SMA-QZSI, QZSI, and Linear Systems

Figure 4 compares the damping ratio $\zeta=0.15$, Base Excitation $\eta=0.2$, stiffness ratio of SMA spring $\alpha_2=0.2$, yield displacement of SMA spring $x_{ms}=0.3$, proportion of initial stiffness of SMA

ISSN: 2710-0588

spring $n = 0.6$, The amplitude frequency response curve and displacement transfer rate curve of SMA-QZSI, QZSI, and linear systems. The results indicate that compared to linear systems, both QZSI and SMA-QZSI systems have smaller resonance frequencies and amplitudes. The resonance amplitude of the amplitude frequency response of the SMA-QZSI system is 37% of that of the linear system, the resonance amplitude of the displacement transfer rate is 46% of it, and the resonance frequency is 50% of it. Compared with the QZSI system, the resonance amplitude of the amplitude frequency response, displacement transfer rate, and isolation starting frequency of the SMA-QZSI system are relatively small. The resonance amplitude of the amplitude frequency response is 78% of that of the QZSI system, the resonance amplitude of the displacement transfer rate is 77% of that of the QZSI system, and the resonance frequency is reduced by 21%. Prove that the system has better isolation performance compared to ordinary three spring isolation systems.

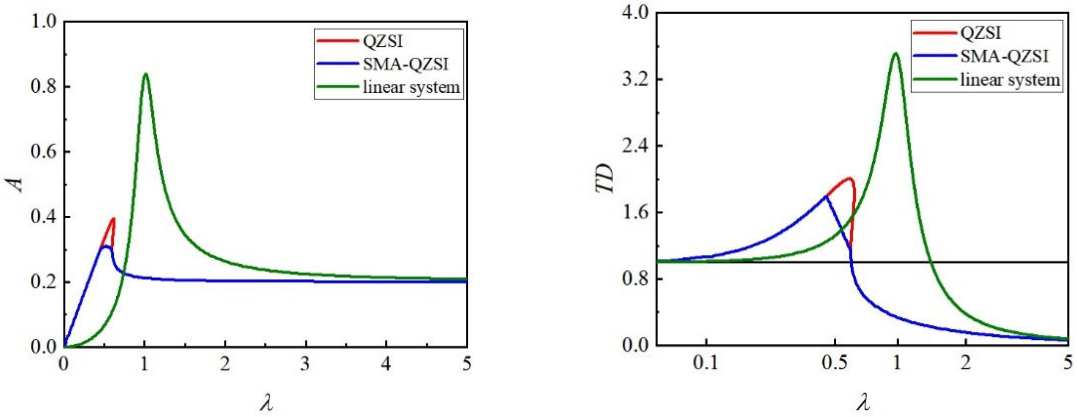

(a) amplitude frequency response (b) displacement transfer rate

Figure 4. QZSI, Comparison of Vibration Isolation Performance between SMA-QZSI and Linear Systems

3.4. The influence of different parameters on the isolation performance of the system

According to formulas (9) and (10), it can be seen that both the amplitude frequency response and displacement transfer rate curves are affected by ζ, η, α_2, n and x_{ms} the impact. Figures 5-9 respectively investigate the effects of changing different parameters on the isolation performance of the system.

3.4.1. Effects of Changing n on Vibration Isolation Performance

The variation pattern of the system curve under the condition of changing n while keeping other parameters constant is shown in Figure 5. As n increases, the resonance peak gradually decreases, especially when n is less than 0.1, the decrease in amplitude frequency response resonance peak and transmission rate peak is particularly significant, indicating that increasing the proportion of a small number of SMA springs is more helpful in improving the isolation performance of the system.

ISSN: 2710-0588

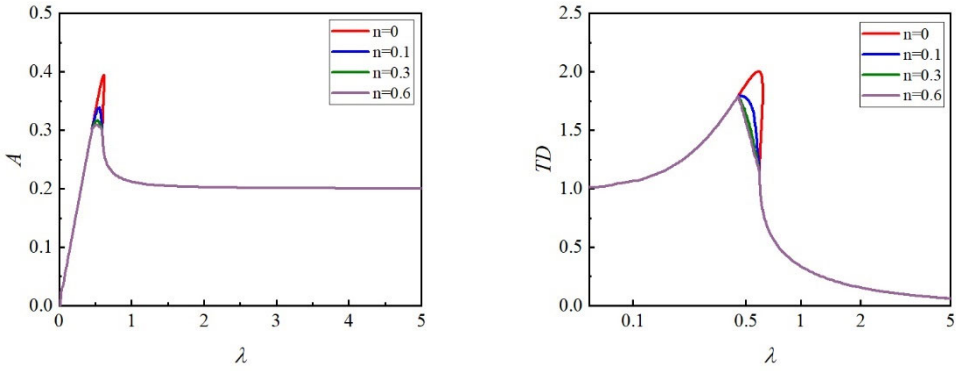

(a) amplitude frequency response (b) displacement transfer rate

Figure 5. The influence of different n values on the isolation performance of the system

3.4.2. Effects of Changing α_2 on Vibration Isolation Performance

Under other constant parameter conditions, the variation pattern of the impact of changing α_2 on the system curve is shown in Figure 6. As the α_2 decreases, the resonance peak of the amplitude frequency response gradually increases, and the value of displacement transfer rate decreases more rapidly after the peak, indicating that the isolation effect gradually improves. Therefore, reducing the stiffness of the second section of the SMA spring is more conducive to enhancing the isolation performance of the system.

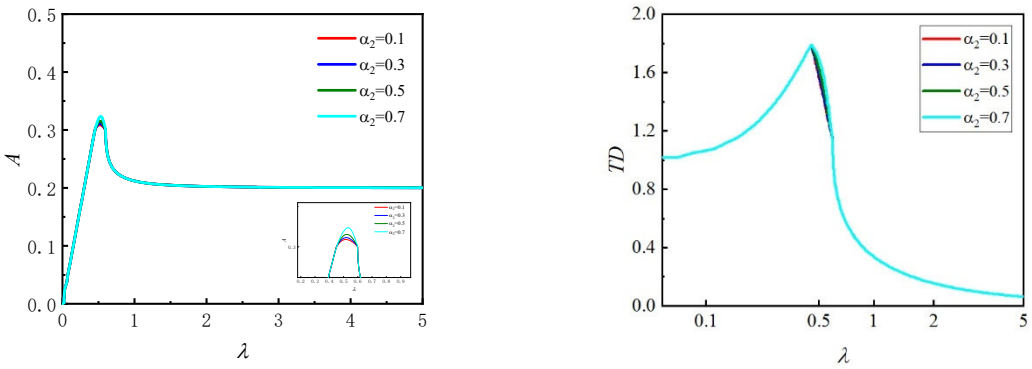

(a) amplitude frequency response (b) displacement transfer rate

Figure 6. The influence of different α_2 values on the isolation performance of the system

3.4.3. Effects of Changing x_{ms} on Vibration Isolation Performance

Under other constant parameter conditions, the variation pattern of the impact of changing the parameter x_{ms} on the system curve is shown in Figure 7. From the graph, it can be seen that the smaller the value of parameter x_{ms}, the more the amplitude frequency response and displacement transfer rate of the system reach their peak values at smaller frequencies, and the peak values are smaller. This indicates that changing the SMA spring to enter the second stage stiffness as soon as possible is more conducive to enhancing the isolation performance of the system.

ISSN: 2710-0588

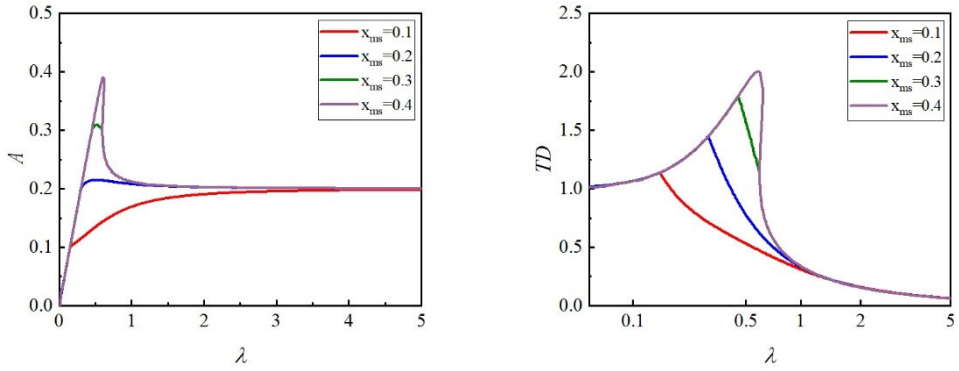

(a) amplitude frequency response (b) displacement transfer rate

Figure 7. The influence of different x_{ms} values on the isolation performance of the system

3.4.4. Effects of Changing ζ on Vibration Isolation Performance

Under other constant parameter conditions, the variation pattern of the impact of changing the parameter ζ on the system curve is shown in Figure 8. From the graph, it can be seen that as ζ increases, the peak values of amplitude frequency response resonance and displacement transfer rate gradually decrease, indicating that increasing the damping ratio appropriately can help improve the isolation performance.

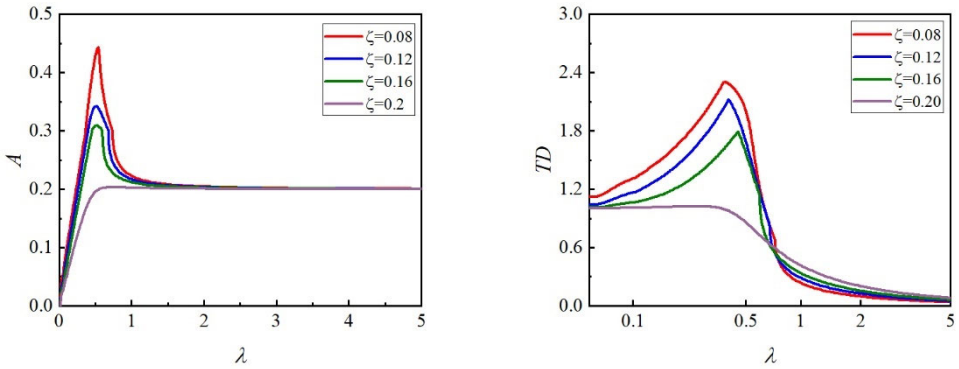

(a) amplitude frequency response (b) displacement transfer rate

Figure 8. The influence of different ζ values on the isolation performance of the system

3.4.5. Effects of Changing η on Vibration Isolation Performance

Under other constant parameter conditions, the variation of the system curve by changing the parameter η is shown in Figure 9. From the graph, it can be seen that as the η increases, the resonance peak gradually increases, and the peak of the transmission rate becomes larger and then decreases more slowly. Moreover, with different η values, the amplitude of the high-frequency stable amplitude response also varies, indicating that the system has better isolation performance under small displacement excitation.

ISSN: 2710-0588

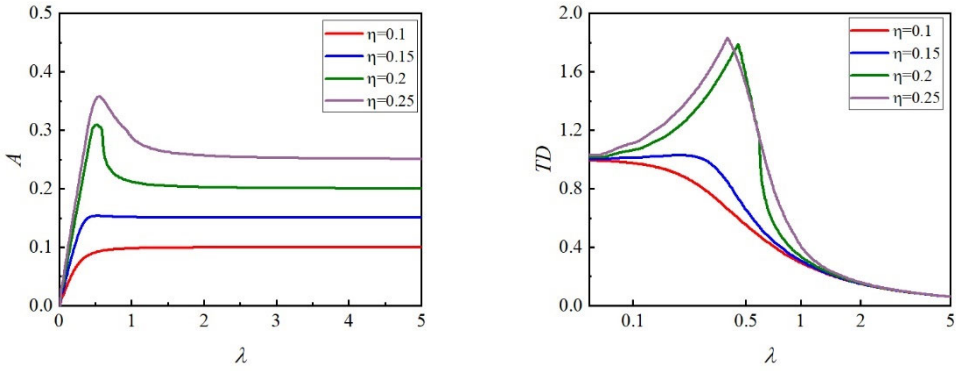

(a) amplitude frequency response (b) displacement transfer rate

Figure 9. The influence of different η values on the isolation performance of the system

3.5. Experimental verification

3.5.1. Parameter Design of Vibration Isolator Prototype

To verify the vibration isolation performance of SMA-QZSI, a prototype of the vibration isolator was made and subjected to vibration table testing. The ordinary compression spring material in the experimental model is spring steel; The SMA spring used is a NiTi alloy SMA spring produced by Xi'an Saite Development Co., Ltd. Zhang Zhenhua et al. [16] conducted loading and unloading tests on this material. The mass block is processed into 6kg, and the vertical compression spring stiffness is k_a =1.2N/mm, SMA spring k_{sm1} is 1.8N/mm,lateral compression spring stiffness k_s is 3N/mm. To ensure the quasi zero stiffness condition of the seismic isolator, it can be obtained that a =44mm, L =66mm.

3.5.2. Test Plan

This experiment mainly uses a sweep frequency test under sinusoidal excitation to obtain the amplitude frequency response of the isolation system, and then determines the displacement transfer rate of the system. Through the system's standing frequency test, the time history response of the system under different excitation frequencies is obtained to verify the isolation performance of the system. Mainly includes:

(1) Conduct tests with excitation displacements of 4mm, 6mm, and 8mm within the frequency range of 2-10 Hz using a vibration table, and record the test data.

(2) Under the condition of an excitation displacement of 6mm, dynamic tests were conducted at excitation frequencies of 3 Hz, 5 Hz, and 7 Hz, and data was recorded.

Figure 10. Physical and experimental site of quasi zero stiffness isolator

ISSN: 2710-0588

3.5.3. Test conditions and result analysis

The vibration isolator was tested within the frequency range of 2-10 Hz with excitation displacements of 4mm, 6mm, and 8mm. The test results are shown in Figure 11. From the graph, it can be seen that as the excitation displacement increases, the peak value of the transmission rate at resonance will increase, but then quickly decrease, demonstrating the good isolation performance of the isolator. From the figure, it can be seen that there is not much time difference between the peak transmission rate when the excitation is 4mm and when the excitation is 6mm, which is caused by friction between the components. When the excitation amplitude is small, the transverse spring fails to provide good negative stiffness at low frequencies.

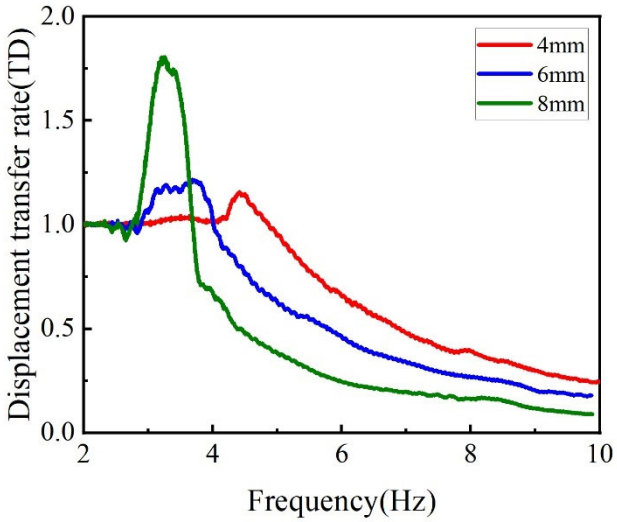

Figure 11. Displacement transmission rate curve under different excitation displacements

Then, different frequency stationary frequency tests were conducted on the isolator, and the test results are shown in Figure12. From the graph, it can be seen that as the frequency increases, the range of displacement changes rapidly decreases, and the peak value of the 3Hz-7Hz transmission rate decreases by 63%, indicating that the isolation performance of the isolator is relatively excellent.

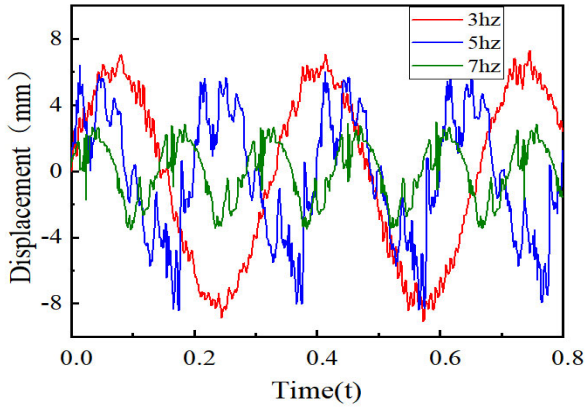

Figure 12. Time history curves at different frequencies

ISSN: 2710-0588

4. Conclusion

This article utilizes the high static and low dynamic characteristics of quasi zero stiffness isolators, the mechanical properties of SMA springs with pseudo elasticity, and the construction of classical three springs to design an SMA-QZSI. And establish a dynamic model of the isolator, derive equations for amplitude frequency response and displacement transfer rate. Next, process the SMA-QZSI components and conduct dynamic tests on a vibration table to verify their vibration isolation performance. Draw the following conclusion:

(1) Perform vibration isolation performance analysis on SMA-QZSI and compare it with linear isolators and classical three spring quasi zero stiffness isolators. The results showed that compared with the QZSI system and its corresponding linear system, the resonance amplitude and frequency in the amplitude frequency response and displacement transfer rate of the SMA-QZSI system decreased. However, compared with the QZSI system, the resonance amplitude of the amplitude frequency response of the SMA-QZSI system decreased by 22%, the common amplitude value of the displacement transfer rate decreased by 23%, and the resonance frequency decreased by 21%. This indicates that the force transmitted to the structure is smaller, further verifying the excellent low-frequency vibration isolation performance of SMA-QZSI.

(2) By processing the isolator model and conducting vibration table tests, the changes in transmission rate when the excitation displacement changes under a predetermined excitation frequency were studied; And with an excitation displacement of 6mm, the time history curve of the isolator was changed by changing the excitation frequency. Both experimental results showed excellent isolation performance of the isolator.

References

[1] Zhang J. Research on Low Frequency Vibration and Active Control of Large Power System Shaft System [J]. Journal of chinese society of power engineering, 2004, (04): 457-460, 465.

[2] Jing X,Yu W,Li Q. Design of a quasi-zero-stiffness based sensor system for the measurement of absolute vibration displacement of moving platforms[J], 2016.

[3] Molyneux,W. G. The Support of an Aircraft for Ground Resonance Tests: A Survey of Available Methods[J], 1958.

[4] Alabuzhev PM,Rivin EI. Vibration protecting and measuring systems with quasi-zero stiffness[J].

[5] Platus DL. Negative-stiffness-mechanism vibration isolation systems[J], 1999.

[6] Peng X, Zhang CX. Static and linear dynamic characteristics analysis of a quasi zero stiffness isolation system [J]. Chinese Quarterly of Mechanics, 2012, 33(03): 492-498.

[7] Peng X, Cheng S. Preliminary exploration of the working principle and application of negative stiffness [J]. Journal of hunan university (Natural Sciences), 1992, (04): 89-94.

[8] Peng X, Li DZ. Design of quasi zero stiffness isolator and its elastic characteristics [J]. Journal of Vibration, Measurement & Diagnosis, 1997, (04): 44-46.

[9] Lee CM,Goverdovskiy VN,Samoilenko SB. Prediction of non-chaotic motion of the elastic system with small stiffness[J], 2004.

[10] Virgin LN,Santillan ST,Plaut RH. Vibration isolation using extreme geometric nonlinearity[J], 2008.

[11] Hang JS, Song JG. Analysis of Nonlinear Isolation Characteristics of a Surface Spring Roller Mechanism [J], 2019.

[12] Carrella A,Brennan MJ,Waters TP. Static analysis of a passive vibration isolator with quasi-zero-stiffness characteristic[J], 2007.

[13] Carrella A,Brennan MJ,Waters TP. On the design of a high-static-low-dynamic stiffness isolator using linear mechanical springs and magnets. [In special Issue: EUROMECH colloquium 483, Geometrically non-linear vibrations of structures][J], 2008.

ISSN: 2710-0588

[14] Tengfei Chen,Yuxuan Zheng,Linhui Song, et al. Design of a new quasi-zero-stiffness isolator system with nonlinear positive stiffness configuration and its novel features[J]. Springer Science and Business Media Llc, 2022, 111(6): 5141-5163.

[15] Qiang Wang,JiaXi Zhou,Kai Wang, et al. Design and experimental study of a compact quasi-zero-stiffness isolator using wave springs[J]. Springer Science and Business Media Llc, 2021, 64(10): 2255-2271.

[16] Zhang Z,Feng L,Sheng P, et. al. A modified one-dimensional constitutive model of pseudoelastic SMAs and its application in simulating the force-deformation relationship of SMA helical springs[J], 2020.